



**HAL**  
open science

## Kinetic analysis of the thermal decomposition of a carbon fibre-reinforced epoxy resin laminate

Pauline Tranchard, Sophie Duquesne, Fabienne Samyn, Bruno Estebe, Serge Bourbigot

► **To cite this version:**

Pauline Tranchard, Sophie Duquesne, Fabienne Samyn, Bruno Estebe, Serge Bourbigot. Kinetic analysis of the thermal decomposition of a carbon fibre-reinforced epoxy resin laminate. *Journal of Analytical and Applied Pyrolysis*, 2017, 126, pp.14 - 21. 10.1016/j.jaap.2017.07.002 . hal-01697363

**HAL Id: hal-01697363**

**<https://hal.science/hal-01697363>**

Submitted on 31 Jan 2018

**HAL** is a multi-disciplinary open access archive for the deposit and dissemination of scientific research documents, whether they are published or not. The documents may come from teaching and research institutions in France or abroad, or from public or private research centers.

L'archive ouverte pluridisciplinaire **HAL**, est destinée au dépôt et à la diffusion de documents scientifiques de niveau recherche, publiés ou non, émanant des établissements d'enseignement et de recherche français ou étrangers, des laboratoires publics ou privés.



Distributed under a Creative Commons Attribution - NonCommercial - NoDerivatives 4.0 International License



## Kinetic analysis of the thermal decomposition of a carbon fibre-reinforced epoxy resin laminate



Pauline Tranchard<sup>a</sup>, Sophie Duquesne<sup>a</sup>, Fabienne Samyn<sup>a</sup>, Bruno Estèbe<sup>b</sup>, Serge Bourbigot<sup>a,\*</sup>

<sup>a</sup> Univ.Lille, UMR 8207, UMET, Unité Matériaux et Transformations, F 59 000 Lille, France

<sup>b</sup> Thermal Expert, ESCSAT, AIRBUS Opération S.A.S, 316 Route de Bayonne – 31060 Toulouse, France

### ARTICLE INFO

#### Keywords:

Thermal decomposition  
Aeronautical CFRP  
TG-FTIR-Thermokinetics  
Kinetic of multi-step reactions

### ABSTRACT (150 MOTS)

Kinetic decomposition model of a carbon-reinforced epoxy laminate (T700/M21 composite) applied to aircraft structures were determined from specific techniques. Data obtained from the thermogravimetric (TG) experiment coupled with Fourier Transform Infrared (FTIR) spectrometer and combined with the NETZSCH Thermokinetics numerical tool were used to determine a comprehensive kinetic model. Experimental and numerical approaches were thus coupled to determine the decomposition mechanism of a partially unknown composite (T700/M21). Using Thermokinetics, a multi-step reactions kinetic model was established based on the TG and differential thermogravimetric (DTG) results. It is composed of two main competitive reaction, e.g.  $n^{\text{th}}$  order and autocatalytic reactions). New approach combining TG-FTIR-Thermokinetics is proposed to make kinetic analysis of complex carbon fibre reinforced epoxy composite (mixture of epoxy resins blended with different thermoplastic polymers).

### 1. Introduction

Combustion depends on processes occurring in both condensed and gas phases. These processes strongly depend on the decomposition reactions occurring in the condensed phase and kinetic analysis permits to model the overall decomposition of a material taken into account multi-step processes (if any). Note that those steps can be independent, parallel, competitive or consecutive. This approach provides the decomposition pathway of the material studied. This work is devoted to the thermal decomposition of a carbon fibre/epoxy laminate. Some papers deal with this topic [1,2], but they are not enough comprehensive to achieve a good assessment on the mechanism of degradation of complex carbon fibre reinforced polymer laminate such as T700 carbon fibre reinforced M21 epoxy resin composite used as structural aircraft material. One of the particularity of this material is linked to its complex formulation that includes an epoxy resin composed of three types of epoxy, one hardener and blended with two thermoplastic polymer (Table 1).

It was demonstrated that the thermal degradation of an epoxy resin is different from one system to another and generalisation is difficult. The thermal decomposition of a carbon fibre reinforced epoxy based polymer depends on the chemical nature of the hardener, the epoxy monomer and, the type and content of fibres used [1–8]. Moreover, carbon fibre can contain powders or coatings acting as a binder coating

[9] in order to promote adhesion between plies during laminate manufacturing process. Today, there is insufficient information on the T700/M21 composite in the literature but methods exists to characterise the decomposition mechanism of material.

Thermogravimetric (TG) measurements coupled with gas analysers is a powerful technique to characterise the thermal decomposition of materials. These gas analysers such as Fourier transformed infrared spectroscopy (FTIR) or mass spectroscopy (MS) techniques permit to analyse the gases evolved during the thermal decomposition of materials. It gives information on the decomposition pathway of the material. Those techniques were applied in the literature by Ahamad [10] who investigated the thermal decomposition of a diglycidyl ether bisphenol-A (DGEBA) epoxy including thermoplastic phenol formaldehyde resin blends (as it is the case for M21 resin – Table 1). They show that the main gases identified are aliphatic chain ends produce methane, ethylene, propylene, allyl alcohol, acetone and acetaldehyde. The aromatic segments of the polymer also produce phenol, benzene, toluene, *ortho*- and *para*- cresols and phenols. In this study, a comparison between TG curves under an inert and an oxidative atmosphere was performed. They identified how and at which temperature the chemical reactions such as thermo-oxidation of the resin occurs. Finally, they proposed a main mechanism of decomposition.

Furthermore, methodologies to characterise the thermal decomposition of materials permit to determine the main kinetic parameter of

\* Corresponding author.

E-mail address: [serge.bourbigot@ensc-lille.fr](mailto:serge.bourbigot@ensc-lille.fr) (S. Bourbigot).

**Table 1**  
Components of the M21 epoxy resin formulation [2,3,21].

Types/Names		Weight percent contents
<i>Thermoplastic blends</i>		
Polyethersulfone	PES	10–20 wt%
Polyamide 6/Polyamide 12	PA 6/12	3–10 wt% ratio 80%/20%
<i>Hardener</i>		
4,4'-Diaminodiphenyl sulfone	DDS	15–20 wt%
<i>Resin</i>		
Diglycidyl ether bisphenol-F	DGEBF	15–20 wt%
Triglycidyl meta aminophenol	TGMAP	20–30 wt%
Para-glycidyl amine	PGAm	5–15 wt%

decomposition namely “activation energy”. This corresponds to the minimum energy necessary to start a chemical reaction. This parameter depends on the state of decomposition, the pressure and the temperature. Since 1960s, considerable progress was made in the development of mathematical techniques to get appropriate kinetic models [11–17]. Depending on the number of decomposition step and on the study (thermomechanical model [18], lightning strike [19], fire behaviour [2,20]), single-step or multiple-step kinetic models were used and has to be more or less precise. In general, decomposition models of the carbon fibre/epoxy composite are reported in the literature but in most cases, the objectives of the authors were to obtain the best fit between experimental and numerical weight loss curve as explained in previous paper [21]. They do not discuss the physical meaning of the parameters and hence, it is not enough if the purpose is to build a real comprehensive model [2,3,21]. New approaches are necessary today to make it possible.

The objective of this paper is therefore studied the mechanism and kinetic of decomposition of T700/M21. The resulting parameters are used as input data for fire modelling (see in [20]). This work started with an understanding of T700/M21 behaviour when exposed to fire [22]. Then, a three-dimensional model was developed and presented [20] with all input data necessary for the model determined [23]. As kinetic parameters are sensitive parameters, they must accurate and reliable: they are absolutely needed to obtain a suitable fire modelling. Kinetic analysis is presented and fully explained here. Therefore, the first part examine the thermal decomposition of the T700/M21 material to determine its decomposition pathway. Then, the second part is devoted to the kinetic analysis of T700/M21 to determine kinetic parameters and to propose a comprehensive decomposition model.

## 2. Methods

### 2.1. Materials

T700/M21 carbon fibre epoxy composite was supplied by Airbus. This composite was manufactured using unidirectional prepreps with an isotropic stacking ([0/45/90/135]s). The features of the material are summarised in Table 1 (details are elsewhere [22]). The M21 resin is a complex formulation containing three types of epoxy resin (diglycidyl ether bisphenol F – DGEBF, triglycidylether *meta*-aminophenol – TGMAP and *para*-glycidyl amine), one hardener (4,4' – diaminodiphenyl sulfone – DDS) and thermoplastic blends (polyether sulfone – PES and polyamide – PA6/PA12) [24,25]. Table 1 presents the components of M21 epoxy resin formulation, which are partially unknown.

### 2.2. Thermogravimetric analysis

Thermogravimetric analysis were carried out on TA Instruments (TA Q5000 and TA Q600). The balance purge flow was set to 15 mL/min and the sample purge flow (nitrogen) to 50 mL/min. Thin square samples put in open alumina pan underwent a heating from 35 to

1100 °C (Q5000)/1500 °C (Q600) with a heating rate of 5, 10, 20, 50 and 100 °C/min.

### 2.3. Gas phase analysis

To characterise the gases released during decomposition of T700/M21, a Fourier Transform InfraRed (FTIR) spectrometer was used (Nicolet iS10 from Thermo Scientific™). This FTIR spectrometer was coupled with the TG device (Q5000 described previously). The gases released from the material inside the TG device go through a heated transfer line up to the FTIR spectrometer. The transfer line temperature is fixed at 225 °C to avoid the condensation of gases. The infrared spectra have been recorded with the OMNIC software. An infrared spectrum is collected every 8 s during all the experiment in the range of wavenumber: 4000 – 800 cm<sup>-1</sup>. The number of scan is fixed at 8 and the resolution at 4 cm<sup>-1</sup>, in order to have a good compromise between the accuracy of the infrared spectra (sufficient signal to noise ratio) and the frequency of collection (one per minute).

### 2.4. Kinetic analysis

To determine kinetic parameters, numerical models, namely “decomposition kinetic models”, were developed using a least-squares fitting procedure based on TG and/or DTG curves [26]. To identify a kinetic decomposition model, TG measurements at various heating rates are performed [26,27]. The analyses of the decomposition mechanism permit to give a physical sense to the kinetic analysis. From a technical point of view, a kinetic analysis is also a tool for data reduction. From a series of measurements with many data points, a model with few parameters is extracted. Then, these parameters will be used for predictions of reaction progress for given temperature conditions. The predictions can be done for one or several measurements like heating. Depending on the studied material, the decomposition can be highly complex. The complex decomposition has to be first understood before formulating exact analytical expressions. Empirical homogeneous kinetic expressions are used to model the decomposition mechanisms. The thermal decomposition is not reversible and is described by a classical reaction rate (Equ. 1) following an Arrhenius equation:

$$\frac{\partial \alpha}{\partial t} = f(\alpha) A \exp\left(\frac{-E_a}{RT}\right) \quad (1)$$

where  $T$  is the temperature,  $R$  is the universal gas constant,  $\alpha$  is the decomposition degree of the material,  $f(\alpha)$  is a reaction conversion function,  $A$  is the pre-exponential factor and  $E_a$  is the apparent energy of activation. Different functions,  $f$ , exist and correspond to a physical phenomenon. Bourbigot et al. [28] proposed four classes of function: (i) all diffusion kinetic functions, (ii) the phase boundary reaction and reaction order kinetic functions, (iii) the nucleation and nucleus growing kinetic functions and the power law nuclear growth functions. The most used function is based on reaction  $n^{\text{th}}$  order kinetics following Equ. 2

$$f(\alpha) = (1 - \alpha)^n \quad (2)$$

where  $n$  is the reaction order.

The Thermokinetics3 software (NETZSCH, Selb, Germany) was used to calculate kinetic parameters. This software includes the two different approaches namely model-free and model based kinetic analysis [11–17,29]. A method proposed by Moukhina [30] to obtain kinetic parameters is followed here. To summarise, this method consists in creating a kinetic model step by step permitting to select the best model. First, a model-free analysis is performed by using Friedman procedure on thermogravimetric data [14]. It permits to plot the activation energy as a function of the degree of conversion (decomposition) degree, which exhibits one or more reaction steps. If the calculated activation energy is constant as a function of decomposition degree, only one reaction occurs and described by only on kinetic equation

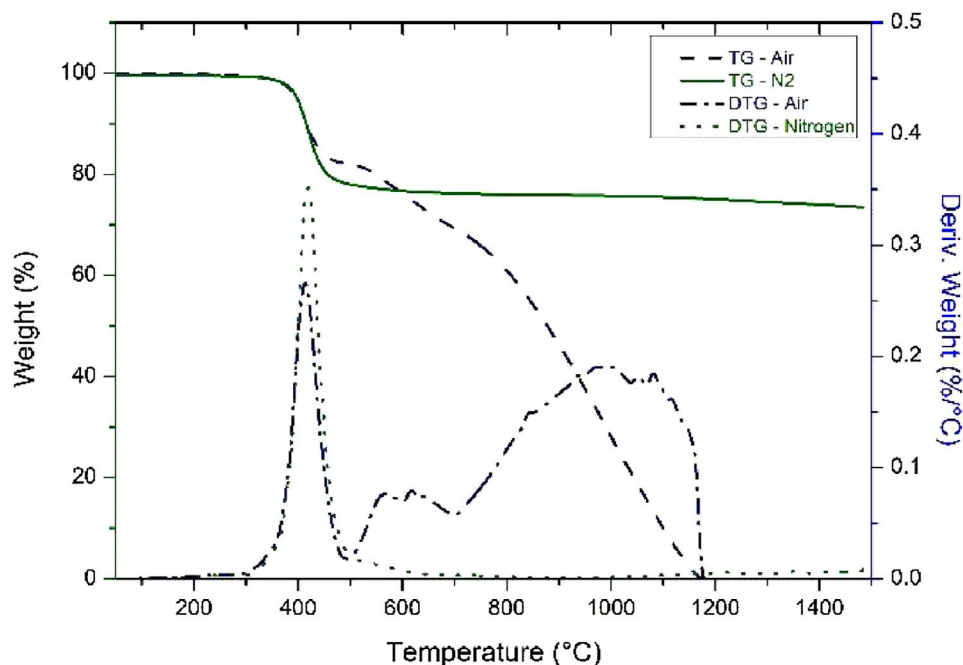


Fig. 1. TG and DTG curves for T700/M21 composite material carried out under nitrogen and air atmosphere at 20 °C/min [2].

(Equ.1). If not, multi-step reactions have to be considered and the reaction rate of each step can be described by an own kinetic equation for this step. In that case, the kinetic model could include independent reactions, consecutive reactions, competitive reactions or a combination of these different reaction types.

### 3. Results and discussion

Using TG-FTIR, the decomposition gases can be identified and the mechanism of decomposition should be elucidated. Our approach is to measure the mass loss of the composite as a function of the temperature under different atmospheres (nitrogen and air) to examine the potential oxidising effect on the decomposition pathway of the composite. Different heating rates are also used to perform the kinetic analysis.

#### 3.1. Thermal decomposition

TG measurements on T700/M21 under nitrogen and under air atmospheres performed at 20 °C/min up to 1500 °C are reported on Fig. 1. TG and differential thermogravimetric (DTG) curves are superimposed to make easier the analysis of the curves.

In inert conditions, only one main peak on the DTG curve is observed corresponding to an apparent step of decomposition. TG curve reaches a plateau at an average mass loss of 26 wt%. Visual observation in the TG pan after the experiment shows that a thermally stable carbonaceous residue was formed. This main step of decomposition is assigned to the decomposition of the resin (M21). Indeed, the T700 carbon fibre has a very small mass loss of 0.8% under nitrogen over the temperature range of 300 – 500 °C (20 °C/min) [31]. According to these authors, this mass loss was attributed to the decomposition of an organic-based sizing compound on the carbon fibre in that range of temperature.

If no interaction between the resin and the carbon fibres are assumed, only the resin can be decomposed. The total weight content of resin is 35 wt% while a 26 wt% weight loss is measured. As a consequence, the formation of carbonaceous residue (small black particles observed in the pan) is assumed. Similar results were found but no explanation was given in the case of M18-1 (27 wt% mass loss whereas the composite is composed of 35 wt% resin [6]). Thus, the decomposition of T700/M21 under nitrogen atmosphere leads to a release of

gases and to the formation of 9 wt% of carbonaceous residue due to the carbonisation of resin. Based on Table 1, it makes sense that the remaining residue is mainly due to: (i) the high amount of char of PES material contained at 10 – 20 wt% in M21 (40 wt% of carbonaceous residue under nitrogen atmosphere [32]); (ii) to the decomposition of the uncrosslinked DDS (40 wt% remaining char at 800 °C under nitrogen atmosphere [33]) and; (iii) to the three epoxy resins [1]. On the contrary, the PA6 is a lower charring material [34] which should not therefore contribute significantly to the formation of the carbonaceous residue. Additional TG measurements on PES and PA6 were done under nitrogen and air atmosphere at 20 °C/min. TG and DTG curves were compared to T700/M21 curves on Fig. 2. Under nitrogen atmosphere (Fig. 2a–c), PA6 does not show any residue after 500 °C and the decomposition of PES occurs in only one-step and at higher temperature than T700/M21 (60 wt% weight loss at 800 °C). Li et al. reported that the decomposition of the epoxy resin under nitrogen atmosphere modified the decomposition of PES when is bended in epoxy/carbon fibre composite [35]. PES blend degraded at the same temperature as the epoxy resin. The effect is the formation of stable carbonaceous residues covering the carbon fibres after the main decomposition step of composite. Therefore, those data permit to conclude that the residue formed from the decomposition of T700/M21 comes from the decomposition of uncrosslinked DDS, PES and epoxies. The stable residue of T700/M21 is thus composed of non-degraded T700 fibre and, of 9 wt% of carbonaceous residue.

Under oxidative atmosphere on Fig. 1b–d), the T700/M21 material totally degrades at high temperature (100% weight loss at 1170 °C). The decomposition of the material occurs in three apparent steps: decomposition of M21 into a carbonaceous residue (1st peak), thermo-oxidation of the intermediate transient carbonaceous residue (2nd peak), and thermo-oxidation of the T700 fibre (3rd peak). To support these comments, additional TG/DTG curves on PES, PA6 and T700 fibre are compared to the TG/DTG results of T700/M21 under air atmosphere at 20 °C/min on Fig. 2c–d). It clearly shows that the decomposition of PES and PA6 were characterised by two successive steps with a second step associated to the char oxidation. This char was totally decomposed after 650 °C for PA6 and 800 °C for PES (confirmed by previous studies [36,37]). Moreover, PA6 seems to degrade during the two first steps of T700/M21 decomposition. For PES, it is assumed chemical interactions between the system carbon fibre/epoxy and PES

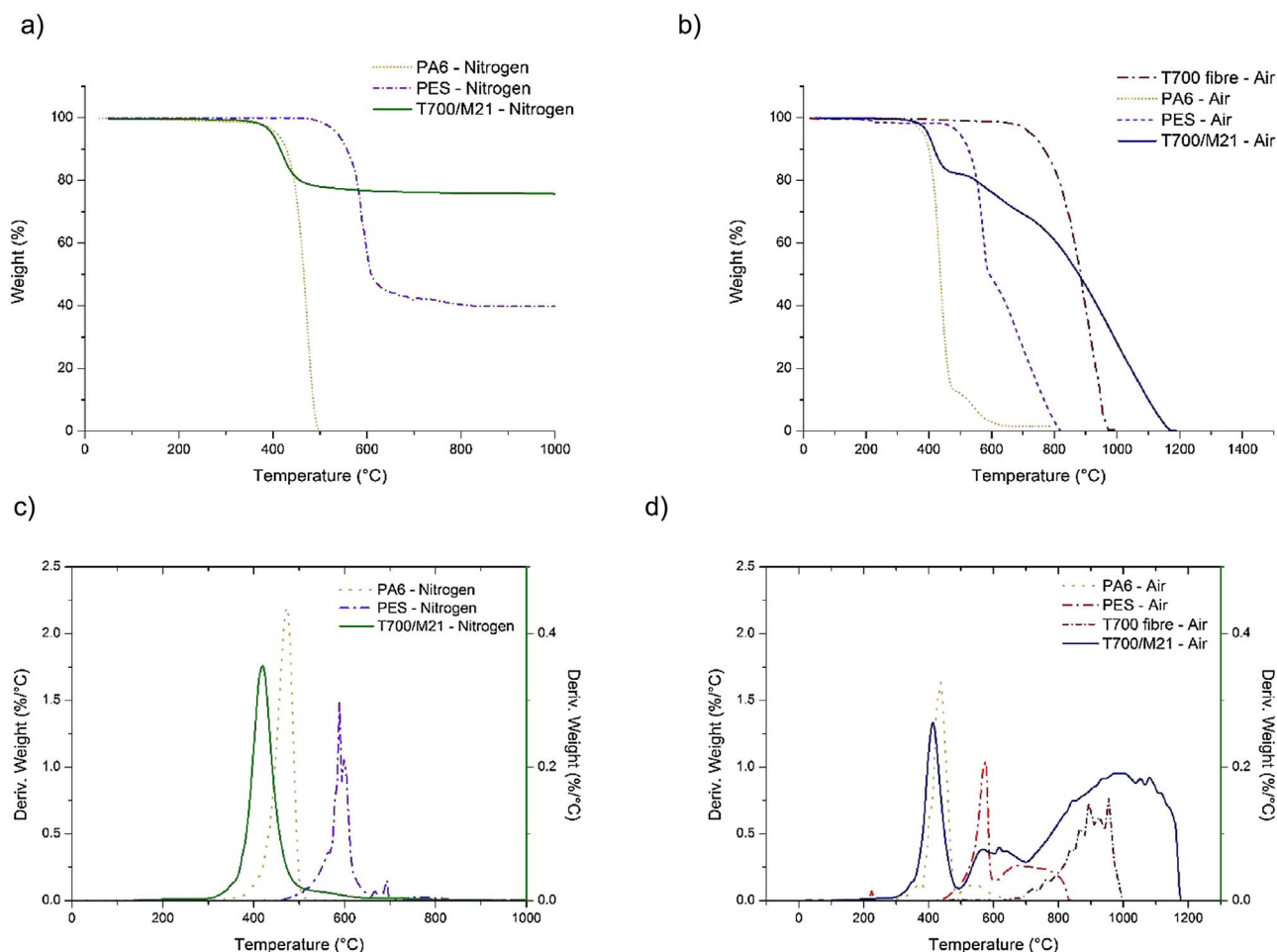


Fig. 2. a) & b) TG and c) & d) DTG curves for T700/M21 composite, PES, PA6 and T700 fibre carried out under nitrogen and air atmosphere at 20 °C/min.

blends during the decomposition of material. As demonstrated by Li et al. [35], the decomposition of the epoxy resin under air atmosphere modified the decomposition of PES when is bended in epoxy/carbon fibre composite. Therefore, PES seems to decompose during the two first steps of T700/M21 decomposition. About the decomposition of T700 fibres, Feih et al. [31] observed that the T700 fibre oxidises over the temperature range of 700–1000 °C which clearly corresponds to the third peak of the weight loss rate observed on Fig. 2d).

The comparison of the TG curves under air and nitrogen atmospheres shows that the oxygen does not influence the decomposition of the resin up to 400 °C (Fig. 1 & 2). The oxygen plays a role in the formation of the transient carbonaceous residue between 400 and 500 °C (plateau observed on the TG curve under air at 18 wt% weight loss compared to 24 wt% weight loss under nitrogen atmosphere which is oxidised in the temperature range of 500–700 °C. Oxygen also plays a role in the decomposition of the carbon fibre in the temperature range 700–1200 °C. In addition, the superposition of both DTG curves shows a common first step of decomposition from 250 °C to 500 °C assigned to the decomposition of M21. Therefore, the decompositions under inert and oxidative atmosphere show respectively one and three apparent steps of decomposition. To go further in the analysis of the decomposition of T700/M21, a gas analysis was carried out to identify the main reactions occurring during the decomposition of the composite.

### 3.2. Gas phase analysis

TG-FTIR permits to characterise the gases released when the material degrades. Fig. 3 shows the main gases released during the decomposition of T700/M21 carried out under nitrogen. Different

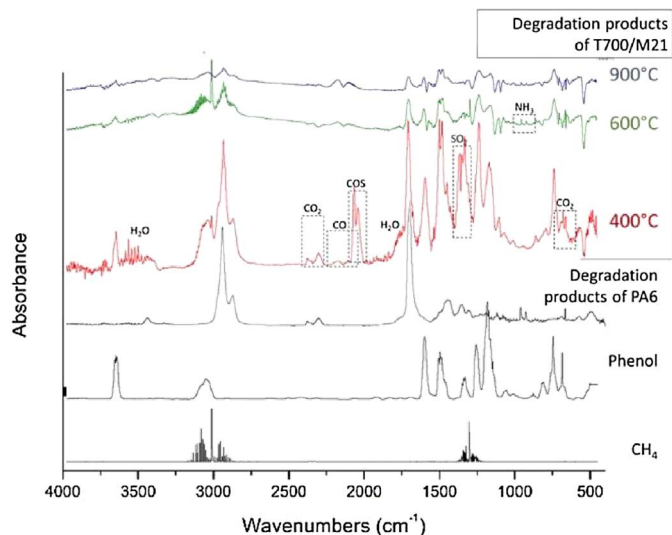


Fig. 3. Spectra collected at 400, 600 and 900 °C of the degradation products of T700/M21 released during TGA (20 °C/min – nitrogen) and of the PA6 (400 °C).

characteristic temperatures were selected (400 °C, 600 °C and 900 °C) corresponding to local maximum of peaks of decomposition observed on DTG curves. The spectra collected at these temperatures are compared and reference spectra are also added on Fig. 3.

In inert atmosphere, water ( $\text{H}_2\text{O}$ : 450–600  $\text{cm}^{-1}$ ; 1250–2000  $\text{cm}^{-1}$ ; 3500–4000  $\text{cm}^{-1}$ ), carbon dioxide ( $\text{CO}_2$ : 3570–3750  $\text{cm}^{-1}$ ;

2300–2400  $\text{cm}^{-1}$ ; 625–725  $\text{cm}^{-1}$ ), carbon monoxide (CO: 2000–2200  $\text{cm}^{-1}$ ), carbonyl sulfide (COS: double peaks at 2070; 2051  $\text{cm}^{-1}$ ), ammonia ( $\text{NH}_3$ : double peaks at 965; 930  $\text{cm}^{-1}$ ) and sulphur dioxide ( $\text{SO}_2$ : 1300–1400  $\text{cm}^{-1}$ ) are released. Moreover, the degradation products of PA6 (mainly the peaks of  $\epsilon$ -caprolactam [37]: 2938  $\text{cm}^{-1}$ ; 1713  $\text{cm}^{-1}$ ), a release of phenol (main peaks: 3652; 1510; 1254; 1170  $\text{cm}^{-1}$ ) and of methane ( $\text{CH}_4$ : 2900–3170  $\text{cm}^{-1}$ ; 1240–1370  $\text{cm}^{-1}$ ) are also observed.

At 400 °C, only traces of  $\text{CO}_2$ , CO and  $\text{NH}_3$  were found, and the main gases identified are  $\text{H}_2\text{O}$ , the degradation products of PA6, phenol,  $\text{CH}_4$ , COS and  $\text{SO}_2$ . The traces of  $\text{CO}_2$ , CO and  $\text{NH}_3$ , and the band  $\epsilon$ -caprolactam are attributed to the decomposition of PA6 under nitrogen [37]. The COS, phenol and the  $\text{SO}_2$  can be released by the decomposition of DDS and/or of PES. According to Rose [38], the decomposition of a TGMDA/DDS at a temperature higher than 310 °C lead to the formation of  $\text{SO}_2$  through a dehydrogenation reaction. Buch [33] also confirmed that the decomposition of DDS leads to the release of  $\text{SO}_2$  and aniline. In our case, the characteristic peak of aniline seems to be hidden by the peaks of phenol. On the other hand, Zhang [39] shows that the major decomposition gases from PES are phenol,  $\text{SO}_2$ ,  $\text{CO}_2$ , CO and a series of aromatic ethers. In addition, the decomposition of a DGEBA/novolac blend (ENB) was studied by Ahamad [10] and the author detected  $\text{H}_2\text{O}$ ,  $\text{CO}_2$ , aliphatic and aromatic hydrocarbons (including  $\text{CH}_4$ ), and of little amount of phenol, of formaldehyde and of CO. At 600 °C, similar peaks are identified compared to the spectrum at 400 °C without the presence of  $\text{H}_2\text{O}$ ,  $\text{CO}_2$  and COS. These decomposition gases can be attributed to the gases evolved during the decomposition of the epoxy and/or DDS, PA6 and PES. At 900 °C, mainly CO is identified but the signal to noise ratio is of the spectrum is too poor to make further comments. The main gases released from the decomposition of T701/M21 identified under nitrogen atmosphere are thus consistent with the results reported in the literature.

Fig. 4 compares the FTIR spectra of the gases collected at the previously defined characteristic temperature when the decomposition is carried out under nitrogen and under air. In oxidative atmosphere, at 400 °C, the peaks corresponding to  $\text{CO}_2$ , CO, COS and  $\text{SO}_2$  are mainly identified as well as some traces of  $\text{H}_2\text{O}$ ,  $\epsilon$ -caprolactam and  $\text{CH}_4$ . At 600 °C and 900 °C, mainly CO and  $\text{CO}_2$  are released under thermo-oxidative atmosphere which evidenced the thermo-oxidative decomposition of the intermediate carbonaceous residue and of the fibre. The release of CO and  $\text{CO}_2$  confirms that this carbonaceous residue as well as the T700 fibre oxidise during the second and the last step of decomposition of the composite. When comparing the results from both atmospheres, differences are clearly observed as from 400 °C. Oxygen plays therefore a main role on the decomposition of the material.

To go further in the analysis, the intensity of the peaks corresponding to the main decomposition products of the composite under nitrogen ( $\epsilon$ -caprolactam, COS,  $\text{SO}_2$ , phenol,  $\text{CH}_4$ ,  $\text{CO}_2$  and CO) are

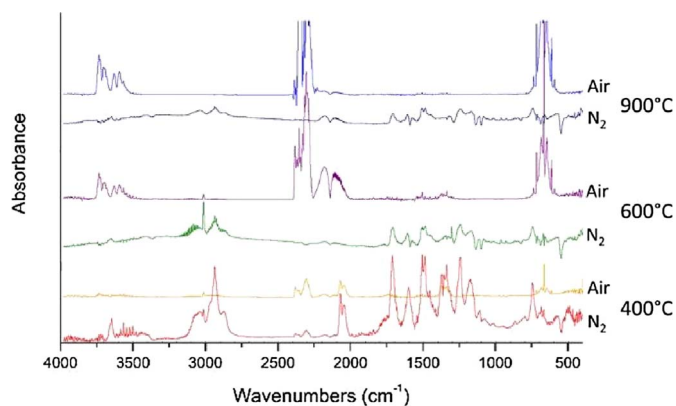


Fig. 4. Infrared spectra at 400, 600 and 900 °C under nitrogen and air during TG measurement of T700/M21 at 20 °C/min [2].

#### Common scale

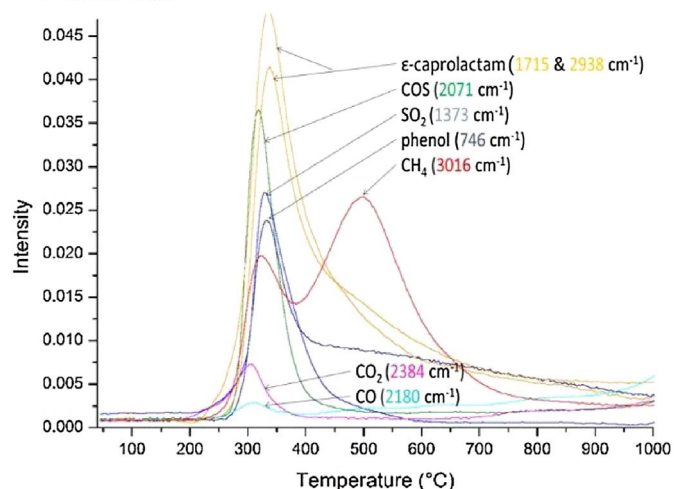


Fig. 5. Intensity curves of  $\epsilon$ -caprolactam, COS,  $\text{SO}_2$ , phenol,  $\text{CH}_4$ ,  $\text{CO}_2$  and CO evolved during the TG experiment of T700/M21 at heating rate of 20 °C/min under nitrogen [2].

plotted as a function of temperature on Fig. 5. It is noteworthy that these data may not be interpreted in a quantitative way and the profiles of peak height of different characteristic peaks are shown using a common scale (to make the comparison easier).

As shown in the previous part, an apparent step from around 300–650 °C can be distinguished on the TG curve of the composite carried out under nitrogen. Fig. 5 shows that the gases released in three main peaks having their maxima at about 350 °C, 500 °C and 1050 °C. The first peaks (maxima at about 350 °C) correspond to the release of all the identified gases. The second maximum (about 500 °C) corresponds to the main evolution of  $\text{CH}_4$  and the third maxima (at about 1050 °C) are due to the evolution of  $\text{CO}_2$  and CO. It can thus be concluded that even under nitrogen atmosphere, three steps of decomposition occur for the T700/M21 composites while they were not detected on TG curves.

To conclude, these results evidence that the decomposition of T700/M21 exhibits at least three steps of decomposition under nitrogen (one main step and two minor steps). Under oxidative atmosphere, three apparent steps occurs and can be attributed to the decomposition of M21 into carbonaceous residue and gaseous decomposition products, thermo-oxidation of this intermediate carbonaceous residue and of T700 occurs at higher temperature. A physical kinetic decomposition model can be thus developed.

#### 3.3. Kinetic decomposition model

The numerical method based on single heating rate measurement cannot be used since the decomposition of T700/M21 is multi-step. TG measurements were carried out at different heating rates (5 °C/min to 400 °C/min from 50 °C to 1000 °C) to determine a decomposition kinetic model of T700/M21 (Fig. 6). In case of a fire, the heating rate can widely vary. Indeed, as shown in previous studies [2,3,22], the temperature at 1 mm from the exposed face at the beginning of the test sharply increases from ambient to 200 °C in less than approximately 20 s (600 °C/min), whereas during the steady state the temperature only slightly varies within the composite. Therefore, the effect of the heating rates on the kinetic parameters must be known over a wide range of conditions. It is noteworthy that only the kinetic decomposition model under nitrogen atmosphere was determined. The assumption is that the decomposition occurs under oxygen depletion when a material is submitted to fire [3,22,40].

TG curves of the composite for various heating rate were compared on Fig. 6. Different observation can be made. For all heating rates, the material seems exhibit only one main step of decomposition. However, the residual mass obtained at high temperature is slightly lower when

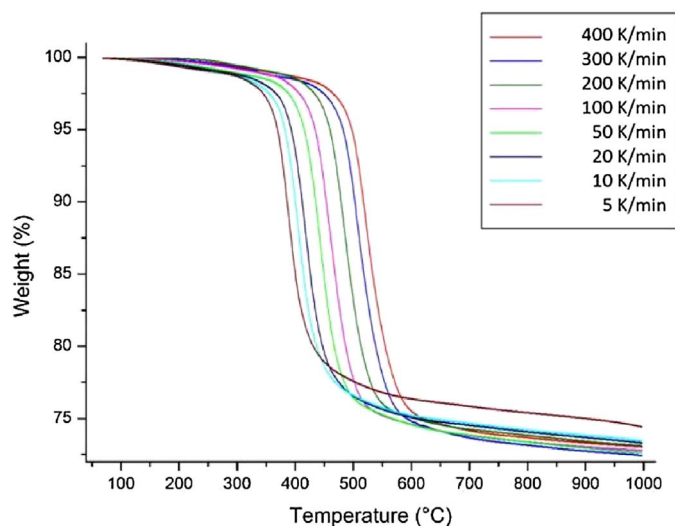


Fig. 6. TG curves for T700/M21 obtained under nitrogen atmosphere at 5, 10, 20, 50, 80, 100, 200, 300 and 400 °C/min [2,3].

the heating rate is higher which suggests competitive reactions. It is reasonable to assume that the material is thermally thin when the heating rates are lower than 100 °C/min (based on calculation of Biot number [2]). Consequently, the kinetic parameters were determined using the TG curves from 5 °C/min to 100 °C/min.

To go further in the analysis, the method proposed by Moukhina [30] was followed to obtain the decomposition model i.e. kinetic parameters. The convenient approach is first to use a model-free analysis as a preliminary step of the kinetic analysis. A model-free analysis (Friedman analysis) provides the plot of the activation energy versus the fractional weight loss (Fig. 7a –  $E_a$  as a function of the decomposition degree – this method requires to calculate an average activation energy for the entire thermal decomposition). It shows that the activation energy is not constant as a function of the decomposition degree and suggests thus a multi-step decomposition as supported by our previous conclusions from the gas phase analysis.

Using the Friedman method, the decomposition degree as a function of the invers of temperature is plotted (Fig. 7b). It permits to compare the slope of the measured curves with the isoconversional lines (black). The experimental points exhibit a higher and similar slopes than the isoconversional lines. Therefore, those results allow identifying mainly an accelerating reaction and a normal reaction.

From the previous discussion, it makes sense to consider two competitive steps to have a model with a physical sense and supported by the experiments. For the accelerating reaction, an autocatalysis reaction is identified using TG-FTIR methods. Indeed, the formation and evolution of  $\text{NH}_3$ ,  $\text{SO}_2$  and  $\text{COS}$  was noted when the gas phase was investigated in previous part. Those gases could play a role of catalysts by promoting the decomposition of T700/M21. Formation of acidic gases during the decomposition of the composite could accelerate the breakup of chains. For example, gases such as  $\text{COS}$  and  $\text{SO}_2$  are used to separate the carbon fibre from the matrix in a composite recycling process [41]. Moreover, the release of  $\text{NH}_3$  can create another catalytic effect such as ammonolysis reaction (uses ammonia to break down the chemical bonds of the epoxy matrix within fibre reinforced composites [42]). These gases released from the epoxy decomposition promote the decomposition of the epoxy resin, which is in accordance with an autocatalytic reaction. So, an autocatalytic reaction was considered for the decomposition of T700/M21. For the normal reaction, it is generally admitted that an  $n^{\text{th}}$  order reaction is considered for the decomposition of material. Finally, the final residues are higher at slow heating rate compared to those at high heating rate (Fig. 6) evidencing competitive reactions. Therefore, multiple reactions occur with at least one competitive reaction being an  $n^{\text{th}}$  order reaction and an

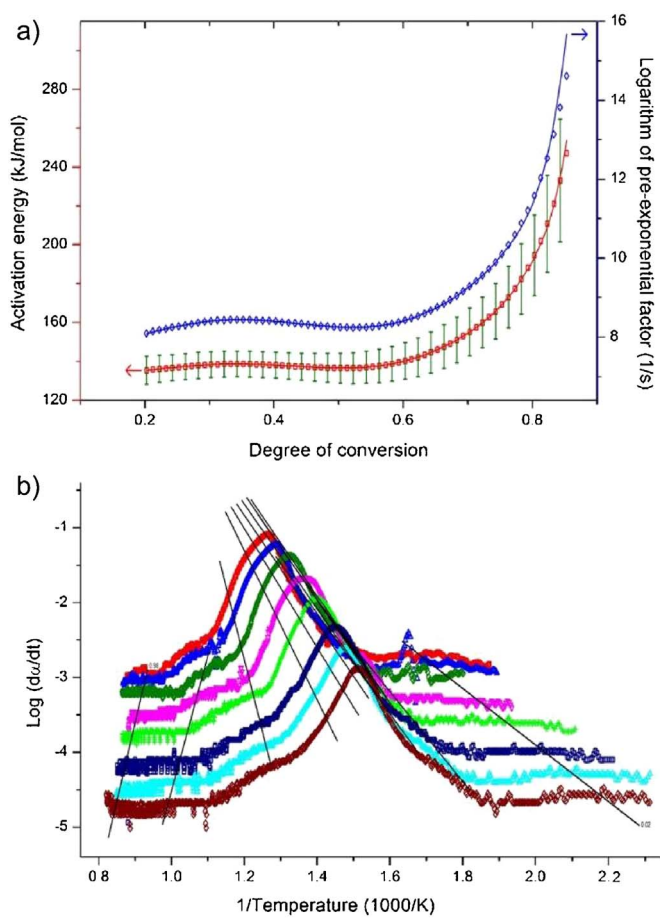


Fig. 7. a) Activation energy as function of fractional mass loss, b) Friedman graphic of T700/M21.

autocatalytic reaction.

Taking into account all these considerations, Fig. 8 shows a comparison between the results obtained from the TG and DTG experiments and from the determined kinetic model (mass loss a) and mass loss rate b)). The kinetic model of each  $i$  steps is presented in Eq. (1–4) and the corresponding kinetic parameters are presented in Table 2.

The main step of decomposition is an autocatalytic step with  $E_a$  equal to 146.7 kJ/mol. This value is consistent with those reported in the literature for other epoxy resins. Indeed, the activation energy for the decomposition of DDS is reported to be equal to 142 ± 15 kJ/mol similar to that of the TGDDM/DDS (147 kJ/mol – 4,4' tetra-glycidyl diamino diphenyl methane) [33]. According to Li et al. [35] the activation energy of a carbon fibre/epoxy and a carbon fibre/epoxy/PES have values of about 120 kJ/mol. PES does not change significantly the activation energy when it is incorporated in an carbon fibre/epoxy composite. In addition, Rose has used the IKP (Invariant Kinetic Parameters) method to determine the parameters  $E_a$  and  $A$  for the kinetic decomposition of the TGDDM/DDS and found values of 125 kJ/mol [38].

The values obtained for the main step of decomposition (step 2) are thus in agreement with the value previously reported in the literature for similar materials and close to the value reported for the DDS decomposition. About the step 1, it is reported that changes in blend structure in the DGEBA-blend modifies their thermal stability, and the activation energy of thermal degradation is in the range 48.3 – 84.5 kJ/mol [38,43]. Hence, the PA6 seems to influence the activation energy. For this reason, the first activation energy (58.7 kJ/mol) of the step 1 is in the same range that its from literature and could be assigned to activation energy of M21 with the PA6 blends.

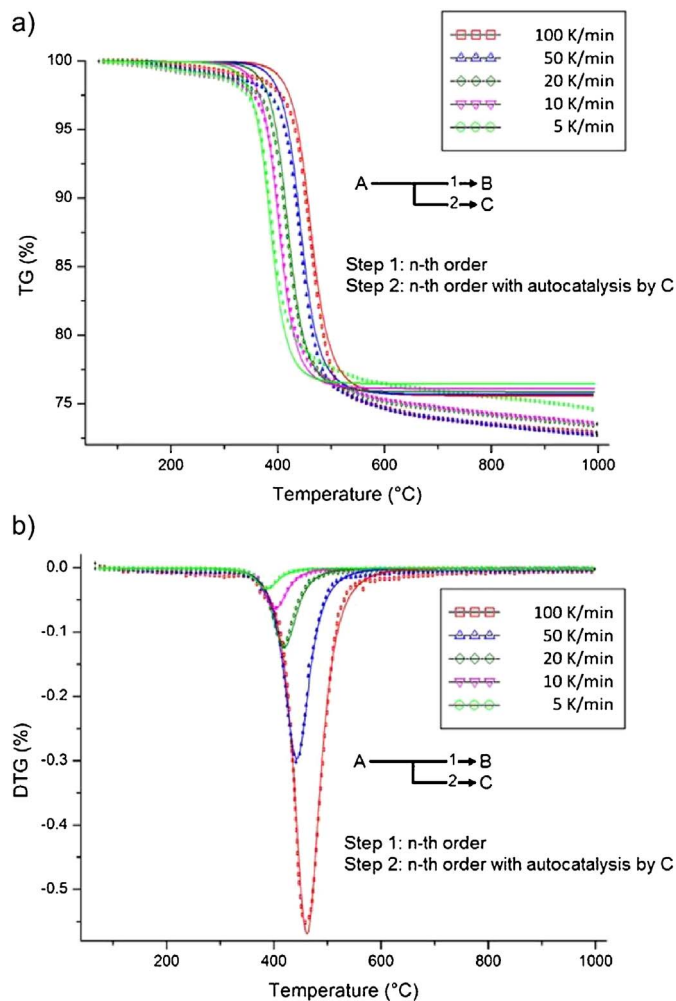


Fig. 8. Comparison of a) TG and b) DTG curves obtained from the experiment (dotted) and from the kinetic decomposition model (plain) for T700/M21 [2].

Table 2  
Kinetic parameters determined for the decomposition of the T700/M21 composite.

Reactions		Step 1	Step 2	Unit
<i>n</i> -th order decomposition				
Activation energy	<i>E<sub>a</sub></i>	58.7	146.7	(kJ/mol)
Frequency	Log <i>A</i>	0.85	8.73	(1/s)
Order	<i>n</i>	1.11	2.08	(–)
Contribution	<i>Fraction</i>	0.55	0.95	(–)
<i>Autocatalysis</i>				
	Log <i>Kcat</i>	–	0.87	(–)

$$\frac{\partial \rho}{\partial t} = - \sum_{i=1}^2 \Delta \rho^i \frac{\partial \alpha_i}{\partial t} \quad (1)$$

where

$$\begin{cases} \frac{\partial \alpha_1}{\partial t} = A_1 (1 - \alpha_1 - \alpha_2)^{n_1} \exp\left(\frac{-E_{a1}}{RT}\right) \\ \frac{\partial \alpha_2}{\partial t} = A_2 (1 - \alpha_1 - \alpha_2)^{n_2} \exp\left(\frac{-E_{a2}}{RT}\right) (1 + Kcat \cdot \alpha_2) \end{cases} \quad (2)$$

and,

$$\rho = \rho_0 - \sum_{i=1}^2 \Delta \rho^i \alpha_i \quad (3)$$

where

$$\begin{cases} \Delta \rho^1 = Fraction1 \cdot (\rho_0 - \rho_e) \\ \Delta \rho^2 = Fraction2 \cdot (\rho_0 - \rho_e) \end{cases} \quad (4)$$

where *t* is the time, *T* is the temperature,  $\rho$  is the density of the material,  $\alpha_i$  is the decomposition degree, *A<sub>i</sub>* is the pre-exponential factor, *E<sub>ai</sub>* is the apparent energy of activation, *n<sub>i</sub>* is the reaction order, *R* is the universal gas constant, the subscripts 0 and *e* correspond to initial and final (end) respectively.

Kinetic analysis permits to propose a model of decomposition supporting the decomposition mechanism determined in the previous part.

#### 4. Conclusions

Thermal decomposition and kinetic analysis of an aeronautical epoxy reinforced carbon fibre composites were investigated. Components of the resin show an interaction in the condensed phase influencing the decomposition of the composite. The decomposition pathways were investigated in details considering the decomposition temperature of each component of the resin and determining, the released gases, and proposing a kinetic decomposition model.

Thermogravimetric measurements and the temperature-related release of decomposition gases of the carbon fibre/epoxy composite were studied by TG-FTIR method. It is shown that the thermal decomposition of the composite occurs in one main step (under inert atmosphere) or three steps (under oxidative atmosphere). The first common step corresponds to the decomposition of epoxy resins, PA6 and PES with the subsequent formation of an intermediate carbonaceous residue. This is able to create a char around T700 fibres. The second step observed under air atmosphere corresponds to the oxidation of this char whereas the last one attributed to the oxidation of T700 carbon fibre.

The main gaseous products released during the composite pyrolysis were identified. In our conditions, the main species released are H<sub>2</sub>O, degradation products of PA6, phenol, CH<sub>4</sub>, COS and CO.

Based on those results, a decomposition model was built up considering two main competitive reactions. The first one is an autocatalytic reaction and the second one, a classical *n*<sup>th</sup>-order reaction.

A comprehensive model was thus obtained using the coupling of TG-FTIR-Thermokinetics methods. It is shown that it is a powerful technique to determine the main mechanism of decomposition of composites including the kinetic decomposition model even if the chemical mechanism of degradation reaction is partially unknown.

#### Acknowledgements

This work was partially supported by Airbus Operation S.A.Sand has received funding from the European Research Council (ERC) under the European Union's H2020-the Framework programme for Research and Innovation (2014–2020)/ERC Grant Advances Agreement n°670747–ERC 2014 AdG/FireBar-Concept.

#### References

- [1] S.V. Levchik, E.D. Weil, Thermal decomposition, combustion and flame-retardancy of epoxy resins—a review of the recent literature, *Polym. Int.* 53 (2004) 1901–1929.
- [2] P. Tranchard, Modelling the Behaviour of a Carbon/epoxy Composite Submitted to Fire, University of Lille, 2015.
- [3] A. Afaghi Khatibi, V. Chevali, S. Feih, A.P. Mouritz, Probability analysis of the fire structural resistance of aluminium plate, *Fire Saf. J.* 83 (2016) 15–24.
- [4] M. Le Bras, N. Rose, S. Bourbigot, The degradation front model – a tool for the chemical study of the degradation of epoxy resins in fire, *J. Fire Sci.* 14 (1996) 199–234.
- [5] E.R. Lyon, A Fire-resistant Epoxy; DOT/FAA/AR-01/53; Federal Aviation Administration (FAA), (2001).
- [6] B. Mortaigne, N. Régnier, Study of epoxy and epoxy-cyanate networks thermal degradation to predict materials lifetime in use conditions, *J. Appl. Polym. Sci.* 77 (2000) 3142–3153.
- [7] A.P. Mouritz, A.G. Gibson, *Fire Properties of Polymer Composite Materials Solid Mechanics and Its Applications* vol.43, (2006) (NY).
- [8] J.P. Firmo, J.R. Correia, L.A. Bisby, Fire behaviour of frp-strengthened reinforced concrete structural elements: a state-of-the-art review, *Compos. Part B-Eng.* 80

- (2015) 198–216.
- [9] F. Lionetto, A. Moscatello, A. Maffezzoli, Effect of binder powders added to carbon fiber reinforcements on the chemoreology of an epoxy resin for composites, *Compos. Part B-Eng.* 112 (2017) 243–250.
- [10] T. Ahamad, S.M. Alshehri, Thermal degradation and evolved gas analysis of epoxy (dgeba)/novolac resin blends (enb) during pyrolysis and combustion, *J. Therm. Anal. Calorim.* 111 (2012) 445–451.
- [11] M.E. Brown, M. Maciejewski, S. Vyazovkin, R. Nomen, J. Sempere, A. Burnham, J. Opfermann, R. Strey, H.L. Anderson, A. Kemmler, et al., Computational aspects of kinetic analysis: part a: the ictac kinetics project-data, methods and results, *Thermochim. Acta* 355 (2000) 125–143.
- [12] A.W. Coats, J.P. Redfern, Kinetic parameters from thermogravimetric data, *Nature* 201 (1964) 68–69.
- [13] J.H. Flynn, The isoconversional method for determination of energy of activation at constant heating rates, *J. Therm. Anal.* 27 (1983) 95–102.
- [14] H.L. Friedman, Kinetics of thermal degradation of char-forming plastics from thermogravimetry: application to a phenolic plastic, *J. Pol. Sci. Part C: Pol. Symp.* 6 (1964) 183–195.
- [15] J. Opfermann, E. Kaisersberger, An advantageous variant of the ozawa-flynn-wall analysis, *Thermochim. Acta* 203 (1992) 167–175.
- [16] T. Ozawa, A new method of analyzing thermogravimetric data, *Bull. Chem. Soc. Jpn.* 38 (1965) 1881–1886.
- [17] J. Šesták, G. Berggren, Study of the kinetics of the mechanism of solid-state reactions at increasing temperatures, *Thermochim. Acta* 3 (1971) 1–12.
- [18] L.A. Burns, S. Feih, P.A. Mouritz, Fire-under-load Testing of Carbon Epoxy Composites 47th AIAA Aerospace Sciences Meeting Including The New Horizons Forum and Aerospace Exposition, Orlando, FL, Orlando, FL, (2009).
- [19] R.D. Chippendale, Modelling of the Thermal Chemical Damage Caused to Carbon Fibre Composites, University of Southampton, 2013.
- [20] P. Tranchard, F. Samyn, S. Duquesne, B. Estèbe, S. Bourbigot, Modelling behaviour of a carbon epoxy composite exposed to fire: part ii—comparison with experimental results, *Materials* 10 (2017) 470.
- [21] P. Tranchard, F. Samyn, S. Duquesne, B. Estèbe, S. Bourbigot, Modelling behaviour of a carbon epoxy composite exposed to fire: part i—characterisation of thermo-physical properties, *Materials* 10 (2017) 494.
- [22] P. Tranchard, F. Samyn, S. Duquesne, M. Thomas, B. Estèbe, J.-L. Montès, S. Bourbigot, Fire behaviour of carbon fibre epoxy composite for aircraft: novel test bench and experimental study, *J. Fire Sci.* (2015).
- [23] ISO2685:1998(E), Aircraft – environmental test procedure for airborne equipment – resistance to fire in designated fire zones, *Int. Organ. Stand. (ISO)* (1998).
- [24] C. Paris, Etude et modélisation de la polymérisation dynamique de composites à matrice thermodurcissable, Graduate Eng. School Univer. Toulouse Toulouse (2011).
- [25] C. Paris, G. Bernhart, P.A. Olivier, O. De Almeida, Influence De Cycles De Cuisson Rapides Sur Le Préimprégné aéronautique m21/t700: Suivi De Polymérisation Et Propriétés mécaniques, (2011).
- [26] J.B. Nelson, Determination of Kinetic Parameters of Six Ablation Polymers by Thermogravimetric Analysis; National Aeronautics and Space Administration: Washington D. C. (1967).
- [27] V. Mamleev, S. Bourbigot, M.L. Bras, J. Lefebvre, Three model-free methods for calculation of activation energy in tg, *J. Therm. Anal. Calorim.* 78 (2004) 1009–1027.
- [28] S. Bourbigot, R. Delobel, M. Le Bras, D. Normand, Comparative study of the integral tg methods used in the invariant kinetic parameter method: application to the fire-retardant polypropylene, *J. Chem. Phys.* 90 (1993) 1909–1928.
- [29] ASTM\_E698, Standard test method for arrhenius kinetic constants for thermally unstable materials using differential scanning calorimetry and the flynn/wall/ozawa method.
- [30] E. Moukhina, Determination of kinetic mechanisms for reactions measured with thermoanalytical instruments, *J. Therm. Anal. Calorim.* 109 (2012) 1203–1214.
- [31] S. Feih, A.P. Mouritz, Tensile properties of carbon fibres and carbon fibre-polymer composites in fire, *Comp. Part A: App. Sci. Manufac.* 43 (2012) 765–772.
- [32] G. Wypych, *Handbook of Polymers*, ChemTec Publishing, Toronto, 2012.
- [33] J.D. Buch, Thermal Expansion Behavior of a Thermally Degrading Organic Matrix Composite ASME Publication AD 04 (1982), pp. 35–49.
- [34] S.V. Levchik, E.D. Weil, M. Lewin, Thermal decomposition of aliphatic nylons, *Polym. Int.* 48 (1999) 532–557.
- [35] C. Li, N. Kang, S.D. Labrandero, J. Wan, C. González, D. Wang, Synergistic effect of carbon nanotube and polyethersulfone on flame retardancy of carbon fiber reinforced epoxy composites, *Ind. Eng. Chem. Res.* 53 (2014) 1040–1047.
- [36] M. Monti, G. Camino, Thermal and combustion behavior of polyestersulfone-boehmite nanocomposites, *Polym. Degrad. Stab.* 98 (2013) 1838–1846.
- [37] M. Coquelle, Flame retardancy of polyamide 6 fibers: the use of sulfamate salts, University of Lille 1, 2014.
- [38] N. Rose, Thermal Degradation and Fire Performance of Epoxy Resins Used in the Aeronautic Industry. Université Lille 1 - Science Et Technologie, (1995).
- [39] H. Zhang, Fire-safe polymers and polymer composites, *Fed. Avia. Adminis. (FAA)* (2004).
- [40] J. Troitzsch, *Plastics Flammability Handbook: Principles, Regulations, Testing, and Approval*, 3rd edition, (2004).
- [41] K. Anderson, A. Sjong, Switchable Ionic Adhesive Coating for Recycle Carbon Fiber, Empire Technology Development Llc, 2012, <http://www.google.com/patents/WO2014035393A1?cl=en>.
- [42] C. Morin, A. Loppinet-Serani, F. Cansell, C. Aymonier, Near- and supercritical solvolysis of carbon fibre reinforced polymers (cfrrps) for recycling carbon fibers as a valuable resource: state of the art, *J. Supercri. Fluids* 66 (2012) 232–240.
- [43] R.H. Patel, V.S. Patel, R.G. Patel, Effect of different epoxy diluents/fortifier on the reactivity in curing and the thermal stability of epoxy resin using 2,2-bis[4-(p-aminophenoxy)phenyl]-propane as a curing agent, *Thermochim. Acta* 141 (1989) 77–86.